

UvA-DARE (Digital Academic Repository)

A new MOF-5 homologue for selective separation of methane from C2 hydrocarbons at room temperature

He, Y.; Song, C.; Ling, Y.; Wu, C.; Krishna, R.; Chen, B.

DOI

[10.1063/1.4897351](https://doi.org/10.1063/1.4897351)

Publication date

2014

Document Version

Final published version

Published in

APL Materials

[Link to publication](#)

Citation for published version (APA):

He, Y., Song, C., Ling, Y., Wu, C., Krishna, R., & Chen, B. (2014). A new MOF-5 homologue for selective separation of methane from C2 hydrocarbons at room temperature. *APL Materials*, 2, 124102. <https://doi.org/10.1063/1.4897351>

General rights

It is not permitted to download or to forward/distribute the text or part of it without the consent of the author(s) and/or copyright holder(s), other than for strictly personal, individual use, unless the work is under an open content license (like Creative Commons).

Disclaimer/Complaints regulations

If you believe that digital publication of certain material infringes any of your rights or (privacy) interests, please let the Library know, stating your reasons. In case of a legitimate complaint, the Library will make the material inaccessible and/or remove it from the website. Please Ask the Library: <https://uba.uva.nl/en/contact>, or a letter to: Library of the University of Amsterdam, Secretariat, Singel 425, 1012 WP Amsterdam, The Netherlands. You will be contacted as soon as possible.

UvA-DARE is a service provided by the library of the University of Amsterdam (<https://dare.uva.nl>)



A new MOF-5 homologue for selective separation of methane from C₂ hydrocarbons at room temperature

Yabing He,^{1,a} Chengling Song,¹ Yajing Ling,¹ Chuande Wu,²
Rajamani Krishna,³ and Banglin Chen^{4,5,b}

¹College of Chemistry and Life Sciences, Zhejiang Normal University, Jinhua 321004, China

²Department of Chemistry, Zhejiang University, Hangzhou 310027, China

³Van't Hoff Institute for Molecular Sciences, University of Amsterdam, Science Park 904, 1098 XH Amsterdam, The Netherlands

⁴Department of Chemistry, University of Texas at San Antonio, One UTSA Circle, San Antonio, Texas 78249-0698, USA

⁵Department of Chemistry, Faculty of Science, King Abdulaziz University, Jeddah 22254, Saudi Arabia

(Received 11 July 2014; accepted 12 August 2014; published online 13 October 2014)

A new MOF-5 homologue compound **UTSA-10** has been obtained under solvothermal conditions from a mixture of Zn(NO₃)₂ · 6H₂O and commercially available linker, 2-methylfumarc acid, in *N,N*-dimethylformamide. The moderate surface area and suitable pore sizes enable the activated **UTSA-10a** to separate methane from C₂ hydrocarbons at room temperature. © 2014 Author(s). All article content, except where otherwise noted, is licensed under a Creative Commons Attribution 3.0 Unported License. [<http://dx.doi.org/10.1063/1.4897351>]

Metal-organic frameworks (MOFs) are a new type of functional porous materials consisting of metal ions or metal containing clusters connected by multidentate organic linkers via metal coordination bonds. By bridging metal ions/clusters with organic linkers, a plethora of compounds with different pore sizes, properties, and functionalities can be systematically designed and synthesized. Compared to conventional porous materials such as zeolites and activated carbons, these hybrid materials have high surface areas and pore volumes, uniform pore sizes, and chemical functionalities. Moreover, their pore sizes and chemical functionalities can be tuned by modifying the metal groups or organic linkers. Hence, MOFs have attracted considerable interest, which has been fueled by the promise of their utilities in gas sorption, separation, heterogeneous catalysis, sensing, and biomedicine.¹⁻¹¹

Nature gas, one of the most important energy resources, mainly consists of methane and also contains small quantities of other hydrocarbons heavier than methane. The removal of these hydrocarbons from natural gas is traditionally carried out by cryogenic distillation, which is very energy-intensive. In contrast, selective adsorption separation near room temperature using porous materials offers an energy-efficient alternative. A few MOF materials have been reported to show the potential for the selective separation of C₂/C₁ hydrocarbons,¹²⁻¹⁷ but the research in this respect is still somewhat limited to date.

MOF-5 (Zn₄O(BDC)₃, BDC = 1,4-benzenedicarboxylate) is a prototypical MOF consisting of a cubic framework built from Zn₄O clusters connected via benzenedicarboxylates.¹⁸ Due to the large surface area, exceptional pore volume, and relatively high thermal stability, it has been widely studied in a variety of fields and usually considered to be a benchmark MOF. Yaghi *et al.* employed isoreticular synthesis method to prepare a series of **MOF-5** homologues with identical topology but diverse porosity and different chemical functionalization.¹⁹ One member of this series exhibited a high capacity for methane storage. Xue *et al.* used a fumaric acid to construct

^aE-mail: heyabing@zjnu.cn

^bE-mail: banglin.chen@utsa.edu. Fax: +1-210-458-7428.



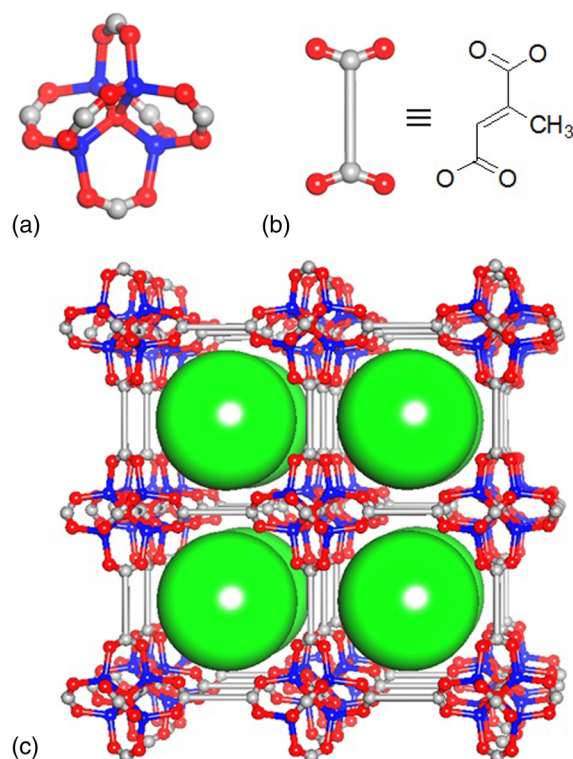


FIG. 1. Schematic representation of the structure of **UTSA-10a** with a cubic framework (c) built from Zn_4O clusters (a) connected via 2-methylfumarate (b).

another **MOF-5** homologue ($Zn_4O(FMA)_3$, FMA = fumarate) exhibiting moderate gas sorption due to comparatively low surface area.²⁰ Herein, we report another prototypical MOF-5 homologue, **UTSA-10**, which is assembled from a readily available dicarboxylate, namely, 2-methylfumarate, in expectation that the methyl group in the organic linker improves the moisture stability and tunes the pore size of the resulting MOF for gas separation application. The activated **UTSA-10a** shows a good potential for the separation of methane from C_2 hydrocarbons at room temperature, which has been comprehensively established by gas sorption isotherms and transient breakthrough and pulse chromatographic simulations.

UTSA-10 was readily synthesized by a solvothermal reaction of 2-methylfumaric acid and $Zn(NO_3)_2 \cdot 6H_2O$ in *N,N*-dimethylformamide (DMF) at 100 °C for 48 h as colorless cubic crystals. The crystal structure was revealed by the similarity of its powder X-ray diffraction (PXRD) pattern to the simulated one from a MOF [$Zn_4O(FMA)_3$]²⁰ that is built from the fumarate ligand of the same length as 2-methylfumarate.²¹ **UTSA-10** adopts a cubic framework structure by connecting $Zn_4O(COO)_6$ clusters with the 2-methylfumarate linkers (Fig. 1). The presence of methyl groups did not interfere with the formation of the isorecticular structure. **UTSA-10** can be formulated as $[Zn_4O(MeFMA)_3] \cdot 8DMF \cdot 2H_2O$ (MeFMA = 2-methylfumarate) on the basis of thermal gravimetric analysis (TGA, supplementary Fig. S1²²) and microanalysis. TGA under a nitrogen atmosphere shows that the desolvated MOF is thermally stable up to 360 °C.

The permanent porosity was unambiguously established by the N_2 sorption isotherm at 77 K. Prior to gas sorption measurement, the as-synthesized **UTSA-10** was guest-exchanged with dry acetone and evacuated under a dynamic vacuum at room temperature for 24 h to generate the activated **UTSA-10a**. Its PXRD pattern matches with that of the pristine sample (supplementary Fig. S2²²), indicating that the structure remains intact after activation. The N_2 sorption isotherm at 77 K shows a characteristic type-I adsorption behavior (Fig. 2), which is typical for microporous materials. **UTSA-10a** can adsorb 282 cm^3 (STP) g^{-1} of N_2 at 77 K. Based on the N_2 adsorption isotherms, the Brunauer-Emmett-Teller (BET) and Langmuir surface areas are calculated to be 1090

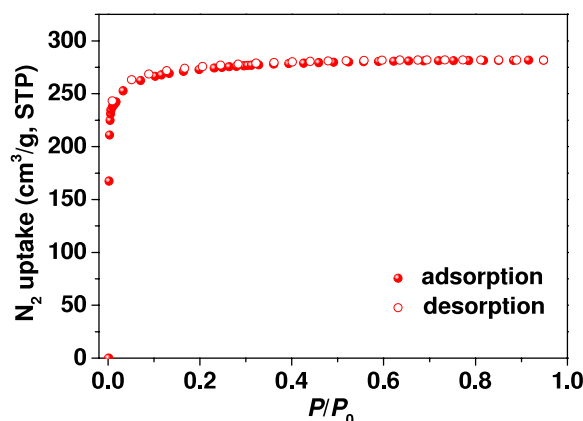


FIG. 2. N_2 sorption isotherm of **UTSA-10a** at 77 K. The solid and open symbols represent the adsorption and desorption data, respectively. STP = Standard Temperature and Pressure.

and $1146 \text{ m}^2 \text{ g}^{-1}$, respectively (supplementary Figs. S3 and S4²²). The total pore volume calculated from the maximum amount of N_2 adsorbed is $0.4358 \text{ cm}^3 \text{ g}^{-1}$. These values are smaller than those of **MOF-5**¹⁸ and $[\text{Zn}_4\text{O}(\text{FMA})_3]$ ²⁰ materials.

We have recently paid much attention to porous MOFs for the storage and separation of small hydrocarbons because of their very important industrial applications.^{12,13,23–30} Given the fact the pore size within **UTSA-10a** tuned by the methyl group in the organic linker falls in the range of the kinetic diameters of C_1 and C_2 hydrocarbons (3.3–4.4 Å), the low-pressure single-component C_2H_2 , C_2H_4 , C_2H_6 , and CH_4 adsorption properties were examined accordingly at two different temperatures of 273 and 296 K. As shown in Fig. 3, all isotherms, except the C_2H_2 one, show good reversible sorption behavior. At 296 K and 1 atm, **UTSA-10a** takes up a negligible amount of CH_4 ($5.8 \text{ cm}^3 \text{ g}^{-1}$), but a moderate amount of C_2H_2 ($43.0 \text{ cm}^3 \text{ g}^{-1}$), C_2H_4 ($31.0 \text{ cm}^3 \text{ g}^{-1}$), and C_2H_6 ($48.5 \text{ cm}^3 \text{ g}^{-1}$). The uptakes of C_2 hydrocarbons are higher than those of **MOF-5**³¹ despite a lower surface area. The higher C_2 hydrocarbon adsorption capacities in comparison with methane indicate that **UTSA-10a** is a very attractive material for the selective adsorptive separation of C_2 hydrocarbons from methane at room temperature.

Based on the pure-component gas sorption isotherms, the Henry's law and IAST (Ideal Adsorbed Solution Theory) selectivities were calculated. The Henry's law selectivities for C_2H_2 , C_2H_4 , and C_2H_6 over CH_4 at 296 K are 8.1, 4.6, and 6.5, respectively, which are moderate compared to those of the best performing MOF materials.¹³ Furthermore, IAST has been applied to calculate adsorption selectivities for an equimolar quaternary $CH_4/C_2H_2/C_2H_4/C_2H_6$ gas mixture in **UTSA-10a** as a function of the total bulk gas phase pressure at 296 K. It was observed from

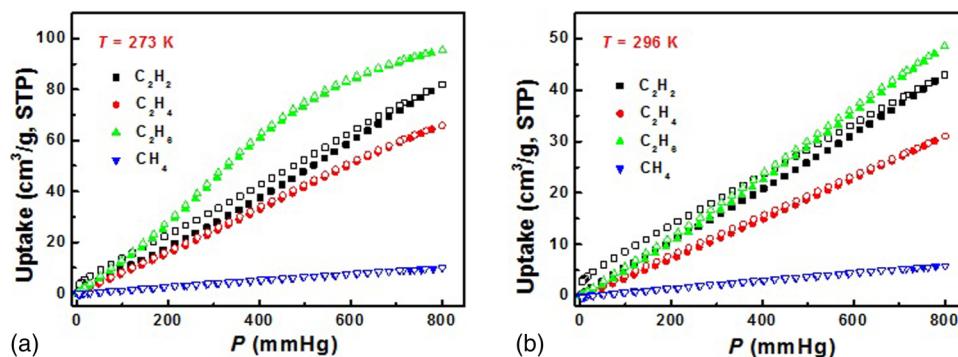


FIG. 3. The single-component C_2H_2 , C_2H_4 , C_2H_6 , and CH_4 sorption isotherms of **UTSA-10a** at 273 K (a) and 296 K (b). The solid and open symbols represent the adsorption and desorption data, respectively.

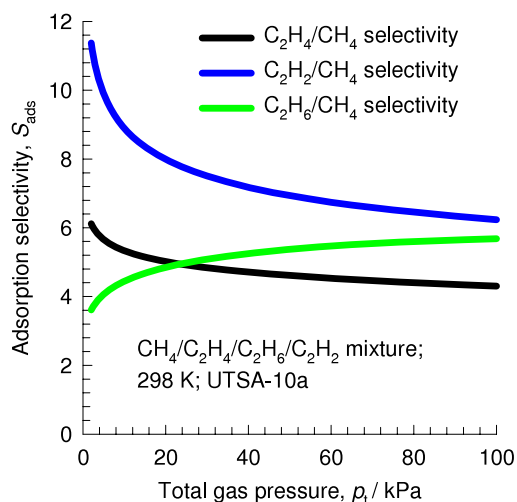


FIG. 4. Calculations using IAST of Myers and Prausnitz³² for C_2H_2/CH_4 , C_2H_4/CH_4 , and C_2H_6/CH_4 selectivities for an equimolar quaternary $CH_4/C_2H_2/C_2H_4/C_2H_6$ gas mixture maintained at isothermal conditions at 296 K using **UTSA-10a**.

Fig. 4 that C_2H_2/CH_4 and C_2H_4/CH_4 selectivities decrease, while C_2H_6/CH_4 adsorption selectivities increase, with increasing pressure. The adsorption selectivities of C_2 hydrocarbons with respect to CH_4 fall in the range of 4–12; this indicates that it is possible to use **UTSA-10a** for selective adsorption of C_2 hydrocarbons from CH_4 .

To understand the separation selectivity, the isosteric enthalpies of adsorption was calculated using the Clausius-Clapeyron equation by fitting the pure-component adsorption isotherms at 273 K and 296 K to a Langmuir-Freundlich expression (supplementary Fig. S5²²). Fig. 5 presents the isosteric enthalpies of adsorption for C_2H_2 , C_2H_4 , C_2H_6 , and CH_4 in **UTSA-10a** as a function of component loadings. Interestingly, the isosteric enthalpies keep constant, independent of surface coverage. The isosteric enthalpy of adsorption of methane is significantly lower and has a value of 13.2 kJ mol^{-1} , whereas the isosteric enthalpy of adsorption of C_2 hydrocarbons has a value of about $19\text{--}27 \text{ kJ mol}^{-1}$. Thus, the preferable adsorption of C_2 hydrocarbons relative to C_1 methane is attributed to the stronger interaction of the framework with C_2 hydrocarbons. Moreover, compared

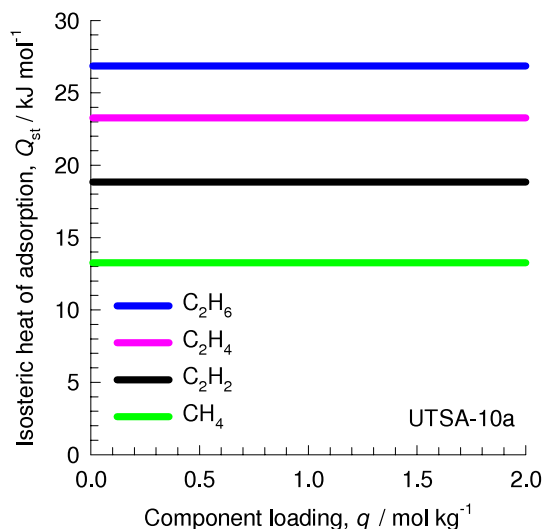


FIG. 5. Comparison of the heats of adsorption of C_2H_6 , C_2H_4 , C_2H_2 , and CH_4 in **UTSA-10a**.

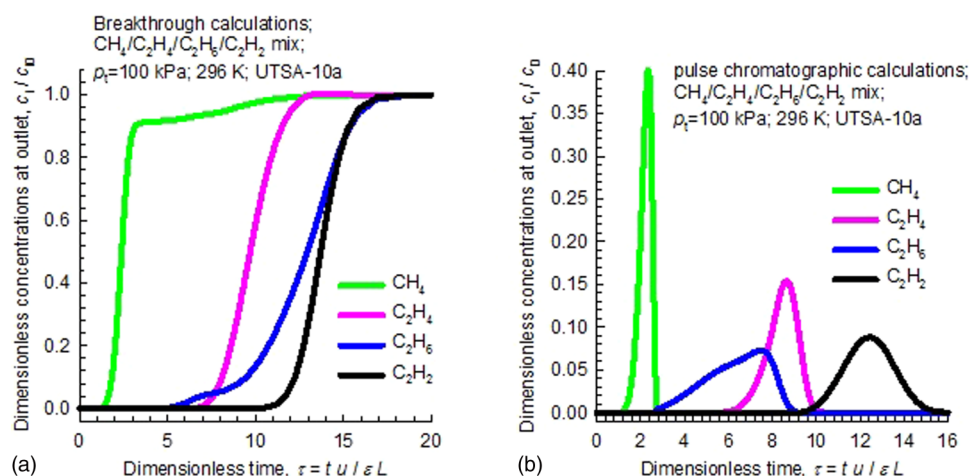


FIG. 6. (a) Breakthrough characteristics of an adsorber packed with **UTSA-10a** maintained at isothermal conditions at 296 K. The inlet gas is an equimolar 4-component quaternary $\text{CH}_4/\text{C}_2\text{H}_2/\text{C}_2\text{H}_4/\text{C}_2\text{H}_6$ gas mixture maintained at isothermal conditions at 296 K and 100 kPa, with partial pressures for each component of 25 kPa. Video animations showing the motion of gas phase concentration fronts traversing the length of the adsorber with an equimolar 4-component $\text{CH}_4/\text{C}_2\text{H}_2/\text{C}_2\text{H}_4/\text{C}_2\text{H}_6$ mixture have been provided as the supplementary material. (b) Pulse chromatographic simulations of an adsorber packed with **UTSA-10a** and maintained at isothermal conditions at 296 K. At the inlet to the adsorber, a pulse of an equimolar 4-component quaternary $\text{CH}_4/\text{C}_2\text{H}_2/\text{C}_2\text{H}_4/\text{C}_2\text{H}_6$ gas mixture is injected for a duration of 10 s.

to the best-performing materials, the low isosteric enthalpy of adsorption indicates the low regeneration cost. It should be pointed out that an ideal adsorbent for gas separation should possess low regeneration cost, besides high uptake capacity and high adsorption selectivity, which need to be equally taken into consideration.

To further demonstrate the separation feasibility, we carried out transient breakthrough and pulse chromatographic simulations following the methodologies of Krishna and Long.^{13,15,24,33,34} The details are provided in the supplementary material. As shown in Fig. 6(a), for an equimolar 4-component gas mixture of C_2H_2 , C_2H_4 , C_2H_6 , and CH_4 maintained at isothermal conditions at 296 K and a total pressure of 100 kPa at the inlet of the adsorber packed with **UTSA-10a**, the sequence of breakthroughs is CH_4 , C_2H_6 , C_2H_4 , and C_2H_2 . There is a significant time interval between the breakthrough of CH_4 and C_2 hydrocarbons. Therefore, it is possible to recover pure methane from this 4-component mixture during the adsorption cycle (see video animations provided in the supplementary material). Fig. 6(b) presents the pulse chromatographic separation of an equimolar 4-component CH_4 – C_2H_2 – C_2H_4 – C_2H_6 mixture with **UTSA-10a** at 296 K. The first peak to emerge from the adsorber is that of methane which can be recovered in nearly pure form. The next sets of peaks are for the C_2 hydrocarbons. Taken together, these simulated data clearly suggest that **UTSA-10a** can effectively separate methane from C_2 hydrocarbons.

In summary, we used a commercially available dicarboxylate to synthesize a new **MOF-5** homologue material, namely, **UTSA-10a**. Gas sorption isotherm measurements and simulated breakthrough studies have comprehensively demonstrated that the MOF has a good potential for the separation of methane from C_2 hydrocarbons at ambient temperature.

This work was supported by an AX-1730 grant from Welch Foundation (BC), the National Natural Science foundation of China (No. 21301156), Open Research Fund of Top Key Discipline of Chemistry in Zhejiang Provincial Colleges, and Key Laboratory of the Ministry of Education for Advanced Catalysis Materials (Zhejiang Normal University, ZJHX201313).

¹ Y. Cui, Y. Yue, G. Qian, and B. Chen, *Chem. Rev.* **112**, 1126–1162 (2012).

² Y. He, W. Zhou, G. Qian, and B. Chen, *Chem. Soc. Rev.* **43**, 5657–5678 (2014).

³ P. Horcajada, R. Gref, T. Baati, P. K. Allan, G. Maurin, P. Couvreur, G. Férey, R. E. Morris, and C. Serre, *Chem. Rev.* **112**, 1232–1268 (2012).

- ⁴ J.-R. Li, J. Sculley, and H.-C. Zhou, *Chem. Rev.* **112**, 869–932 (2012).
- ⁵ L. E. Kreno, K. Leong, O. K. Farha, M. Allendorf, R. P. V. Duyne, and J. T. Hupp, *Chem. Rev.* **112**, 1105–1125 (2012).
- ⁶ H. Wu, Q. Gong, D. H. Olson, and J. Li, *Chem. Rev.* **112**, 836–868 (2012).
- ⁷ S. Kitagawa, R. Kitaura, and S.-i. Noro, *Angew. Chem., Int. Ed.* **43**, 2334–2375 (2004).
- ⁸ M. P. Suh, H. J. Park, T. K. Prasad, and D.-W. Lim, *Chem. Rev.* **112**, 782–835 (2012).
- ⁹ H.-L. Jiang and Q. Xu, *Chem. Commun.* **47**, 3351–3370 (2011).
- ¹⁰ L. Ma, C. Abney, and W. Lin, *Chem. Soc. Rev.* **38**, 1248–1256 (2009).
- ¹¹ Y. Liu, W. Xuan, and Y. Cui, *Adv. Mater.* **22**, 4112–4135 (2010).
- ¹² M. C. Das, H. Xu, S. Xiang, Z. Zhang, H. D. Arman, G. Qian, and B. Chen, *Chem. - Eur. J.* **17**, 7817–7822 (2011).
- ¹³ Y. He, R. Krishna, and B. Chen, *Energy Environ. Sci.* **5**, 9107–9120 (2012).
- ¹⁴ S. Horike, Y. Inubushi, T. Hori, T. Fukushima, and S. Kitagawa, *Chem. Sci.* **3**, 116–120 (2012).
- ¹⁵ E. D. Bloch, W. L. Queen, R. Krishna, J. M. Zadrozny, C. M. Brown, and J. R. Long, *Science* **335**, 1606–1610 (2012).
- ¹⁶ J. Cai, J. Yu, H. Xu, Y. He, X. Duan, Y. Cui, C. Wu, B. Chen, and G. Qian, *Cryst. Growth Des.* **13**, 2094–2097 (2013).
- ¹⁷ J. Jia, L. Wang, F. Sun, X. Jing, Z. Bian, L. Gao, R. Krishna, and G. Zhu, *Chem. - Eur. J.* **20**, 9073–9080 (2014).
- ¹⁸ H. Li, M. Eddaoudi, M. O’Keeffe, and O. M. Yaghi, *Nature* **402**, 276–279 (1999).
- ¹⁹ M. Eddaoudi, J. Kim, N. Rosi, D. Vodak, J. Wachter, M. O’Keeffe, and O. M. Yaghi, *Science* **295**, 469–472 (2002).
- ²⁰ M. Xue, Y. Liu, R. M. Schaffino, S. Xiang, X. Zhao, G.-S. Zhu, S.-L. Qiu, and B. Chen, *Inorg. Chem.* **48**, 4649–4651 (2009).
- ²¹ Single-crystal X-ray crystallographic data: *Fm*3m, $a = b = c = 21.643 \text{ \AA}$, $\alpha = \beta = \gamma = 90^\circ$, $V = 10138 \text{ \AA}^3$.
- ²² See supplementary material at <http://dx.doi.org/10.1063/1.4897351> for thermal gravimetric analysis; powder X-ray diffraction patterns before and after activation; the BET and Langmuir analysis of N₂ adsorption isotherms; and the Langmuir-Freundlich fits of the gas adsorption isotherms.
- ²³ Y. He, W. Zhou, R. Krishna, and B. Chen, *Chem. Commun.* **48**, 11813–11831 (2012).
- ²⁴ Y. He, S. Xiang, Z. Zhang, S. Xiong, F. R. Fronczek, R. Krishna, M. O’Keeffe, and B. Chen, *Chem. Commun.* **48**, 10856–10858 (2012).
- ²⁵ Y. He, Z. Zhang, S. Xiang, F. R. Fronczek, R. Krishna, and B. Chen, *Chem. Commun.* **48**, 6493–6495 (2012).
- ²⁶ Y. He, Z. Zhang, S. Xiang, F. R. Fronczek, R. Krishna, and B. Chen, *Chem. - Eur. J.* **18**, 613–619 (2012).
- ²⁷ Y. He, Z. Zhang, S. Xiang, H. Wu, F. R. Fronczek, W. Zhou, R. Krishna, M. O’Keeffe, and B. Chen, *Chem. - Eur. J.* **18**, 1901–1904 (2012).
- ²⁸ S. Xiang, Z. Zhang, C.-G. Zhao, K. Hong, X. Zhao, D.-L. Ding, M.-H. Xie, C.-D. Wu, R. Gill, K. M. Thomas, and B. Chen, *Nature Commun.* **2**, 204 (2012).
- ²⁹ H. Xu, Y. He, Z. Zhang, S. Xiang, J. Cai, Y. Cui, Y. Yang, G. Qian, and B. Chen, *J. Mater. Chem. A* **1**, 77–81 (2013).
- ³⁰ M. C. Das, Q. Guo, Y. He, J. Kim, J. C.-G. Zhao, K. Hong, S. Xiang, Z. Zhang, K. M. Thomas, R. Krishna, and B. Chen, *J. Am. Chem. Soc.* **134**, 8703–8710 (2012).
- ³¹ S. Xiang, W. Zhou, J. M. Gallegos, Y. Liu, and B. Chen, *J. Am. Chem. Soc.* **131**, 12415–12419 (2009).
- ³² A. L. Myers and J. M. Prausnitz, *AIChE J.* **11**, 121–127 (1965).
- ³³ R. Krishna and J. R. Long, *J. Phys. Chem. C* **115**, 12941–12950 (2011).
- ³⁴ H. Wu, K. Yao, Y. Zhu, B. Li, Z. Shi, R. Krishna, and J. Li, *J. Phys. Chem. C* **116**, 16609–16618 (2012).